Magnetic-Field Dependence of Tunnel Couplings in Carbon Nanotube Quantum Dots

Grove-Rasmussen, Kasper; Grap, S.; Paaske, Jens; Flensberg, Karsten; Andergassen, Sabine; Meden, Volker; Jørgensen, Henrik Ingerslev; Muraki, K.; Fujisawa, T.

Magnetic-Field Dependence of Tunnel Couplings in Carbon Nanotube Quantum Dots

K. Grove-Rasmussen,[1,2,*] S. Grap,[3] J. Paaske,[2] K. Flensberg,[2] S. Andergassen,[3,4] V. Meden,[3] H. I. Jørgensen,[2]
K. Muraki,[1] and T. Fujisawa[1,5]

[1]*NTT Basic Research Laboratories, NTT Corporation, 3-1, Morinosato-Wakamiya, Atsugi 243-0198, Japan*
[2]*Niels Bohr Institute and Nano-Science Center, University of Copenhagen, Universitetsparken 5, 2100 Copenhagen Ø, Denmark*
[3]*Institut für Theorie der Statistischen Physik and JARA-Fundamentals of Future Information Technology,
RWTH Aachen University, 52056 Aachen, Germany*
[4]*Faculty of Physics, University of Vienna, Boltzmanngasse 5, 1090 Wien, Austria*
[5]*Department of Physics, Tokyo Institute of Technology, 2-12-1 Ookayama, Meguro 152-8551, Japan*

By means of sequential and cotunneling spectroscopy, we study the tunnel couplings between metallic
leads and individual levels in a carbon nanotube quantum dot. The levels are ordered in shells consisting
of two doublets with strong- and weak-tunnel couplings, leading to gate-dependent level renormalization.
By comparison to a one- and two-shell model, this is shown to be a consequence of disorder-induced
valley mixing in the nanotube. Moreover, a parallel magnetic field is shown to reduce this mixing and thus
suppress the effects of tunnel renormalization.

PACS numbers: 73.63.Kv, 71.10.−w, 73.63.Fg

Confined states and their tunnel couplings to the leads are
the basis for a wealth of intriguing phenomena observed in
quantum dot nanostructures. In carbon nanotubes, the states
appear in a particularly simple arrangement of near fourfold
degenerate shells stemming from spin and orbital degrees of
freedom [1,2]. The splitting of each quartet into two dou-
blets is well understood within a single particle model,
including disorder-induced valley mixing and spin-orbit
interaction [3,4]. Less is known about the tunnel couplings,
but experiments show that they can be different for the two
doublets within a shell [5]. In a clean nanotube, such be-
havior would be inconsistent with time-reversal symmetry.

In this Letter, we show that the relevant doublets indeed
may have different lead couplings due to orbital disorder,
and that this tunnel coupling asymmetry is tunable by a
parallel magnetic field $B_\parallel$. At $B_\parallel = 0$ T, strong and weak
Kondo effects in the charge stability diagrams and gate-
dependent inelastic cotunneling thresholds indicate differ-
ent doublet couplings [5]. At finite $B_\parallel$, Coulomb peaks
exhibit $B_\parallel$-dependent level broadenings, indicating field-
tunable tunnel couplings, which is further corroborated by
the disappearance of gate-dependent inelastic cotunneling
lines for equal couplings. A single-shell model including
disorder, expressed as an intrashell coupling $\Delta_{KK'}$ between
the orbital states K and K', is shown to account well for the
observed coupling behavior at low fields. At larger $B_\parallel$, the
coupling strengths of the doublets even interchange and
show nonmonotonic behavior, which can be explained by a
two-shell model including an intershell orbital coupling
$\Delta_{KK'12}$ [6]. By applying the functional renormalization
group (fRG) to the inner four levels of the two-shell model,
it is shown that the linear conductance versus gate voltage
V_{gate} is in good agreement with the measurement for all $B_\parallel$
[7], including correlation effects such as Kondo effect.

Figure 1(a) shows a bias spectroscopy plot obtained
by measuring the differential conductance at temperature
$T = 140$ mK of a 400 nm long AuPd contacted single-wall
carbon nanotube device versus source-drain bias and back-
gate voltage [see inset in Fig. 1(a)] [4]. In the V_{gate} range
shown, quantum states belonging to two near-fourfold
degenerate shells in the valence band are filled. This leads
to the characteristic pattern [1] of three smaller faintly
visible diamonds followed by a big (truncated) diamond
as V_{gate} is increased. Inside each diamond, the nanotube
holds an integer number of electrons, N, indicated by the
additional electron number for filled shells. For odd occu-
pancy of the shells, zero-bias conductance ridges are
observed, which is a manifestation of the well-known
spin-half Kondo effect [8,9]. Interestingly, the Kondo
ridges are broad and narrow for $N + 1$ and $N + 3$ electrons
in the shell, respectively. A gate-dependent step in con-
ductance at small finite bias (especially pronounced for
filling $N + 2$ and $N + 3$ in the small diamonds) reveals
the splitting of the four states within a shell into two doublets
via inelastic cotunneling; i.e., at bias voltages correspond-
ing to the doublet energy difference, an electron may
tunnel into the excited doublet provided that an electron
tunnels out from the ground state doublet [10]. Both fea-
tures can be understood by assuming that the two doublets
have different couplings to the leads: a strongly (weakly)
coupled ground (excited) state results in a strong (weak)
Kondo resonance, while gate-dependent level renormaliza-
tions of the doublets are due to charge fluctuations between
the dot and the leads [5,11]. Until now it has remained
unclear how the two doublets could be differently coupled.

To understand the doublet states in more detail, the zero-
bias conductance of a single shell is measured as a function
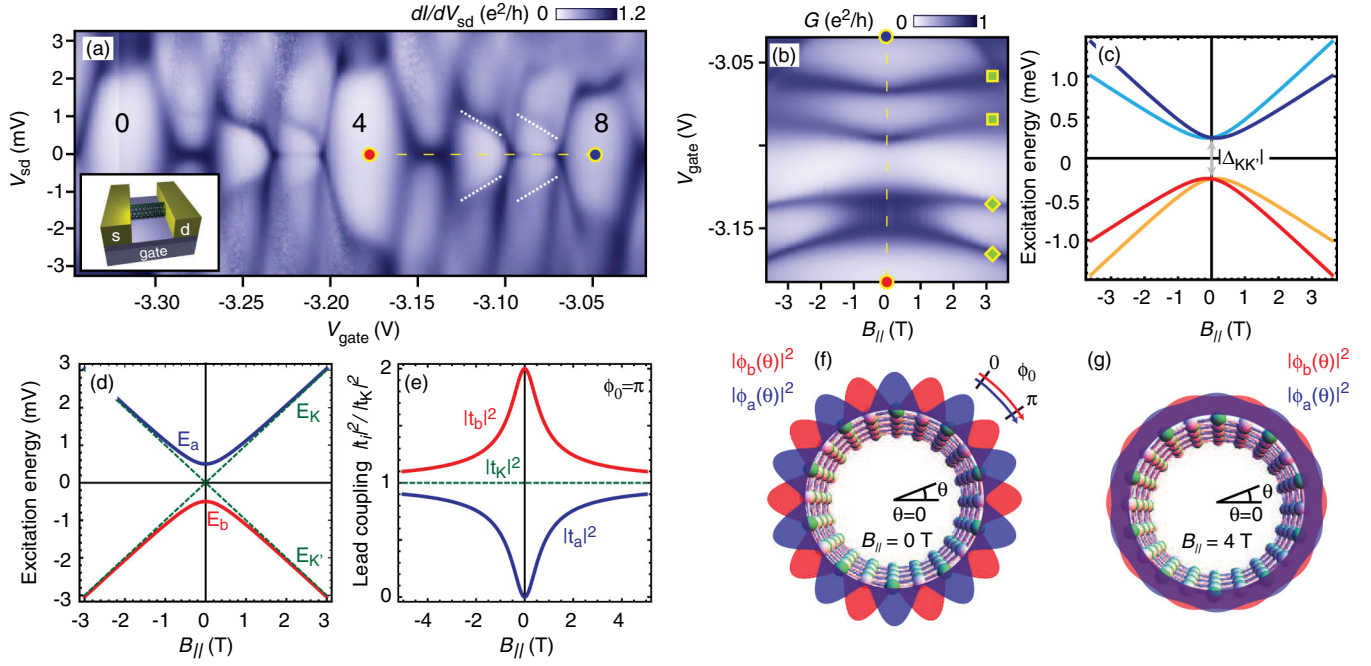of $B_\parallel$, and results are shown in Fig. 1(b) [gate range in

FIG. 1 (color online).   (a) Charge stability diagram of two nanotube shells showing a pattern of strong or weak Kondo effect for odd occupation and gate-dependent inelastic cotunneling thresholds. Inset: backgated two-terminal carbon nanotube device. (b) Linear conductance versus $B_\parallel$ for the V_{gate} region marked by the dashed yellow line in (a). (c) Shell energy diagram showing the eigenenergies in the presence of an orbital coupling $\Delta_{KK'}$. (d),(e) Level energies and level-lead couplings of a simple spinless model. Because of $\Delta_{KK'}$ (with orbital phase $\phi_0 = \pi$), the eigenstates are now differently coupled to the leads at $B_\parallel = 0$, while becoming more equally coupled as $B_\parallel$ is increased. (f),(g) Simple picture showing that the electron probability distributions for the two eigenstates are different (similar) at zero (large) field.

Fig. 1(a) marked by horizontal dashed line]. The upward and downward energy shifts of pairs of Coulomb peaks with increasing field are consistent with expectations from a simple nanotube shell model including intrashell orbital coupling $\Delta_{KK'}$ [12] with energies as shown in Fig. 1(c) [4,6,11]. The lower (red and orange) and upper (blue and cyan) lines are the resulting eigenstates corresponding to a finite intrashell coupling. Moreover, the widths of the Coulomb peaks (increasing with tunnel coupling) emerging from the broad Kondo ridge become narrower as the field is increased (diamonds), while a broadening is observed in the case of the narrow Kondo ridge (squares) [13]. The tunnel couplings to the leads are thus observed to be $B_\parallel$ dependent.

The observed strong and weak tunnel coupling behavior of the doublets is a consequence of the intrashell orbital coupling as can readily be understood from a simple spinless model with level energies shown in Fig. 1(d). Time-reversal symmetry demands that $|t_K| = |t_{K'}| = t$, but in the presence of a finite intrashell orbital coupling, $\Delta_{KK'} = |\Delta_{KK'}|e^{i\phi_0}$, so that the new eigenstates $|b/a\rangle \sim \mp e^{i\phi_0}|K\rangle + |K'\rangle$ at $B_\parallel = 0$ are tunnel coupled by $t(1 \mp e^{i\phi_0})$, respectively [5,11]. For $\phi_0 = \pi$ and $B_\parallel = 0$, one of these states completely decouples from the leads, while the original eigenstates are restored and couplings become equal for $B_\parallel \gg |\Delta_{KK'}|$ [see Fig. 1(e)]. With this picture in mind, the

decrease (increase) in coupling versus field of the strongly (weakly) coupled doublets is readily understood. The model gives a microscopic picture of why the tunnel couplings of the two doublets can be different. It does not, however, address the issue of conserved quantum numbers required for the SU(4) or orbital Kondo effect [6,14,15]. Figure 1(f) shows that the electron density (and therefore tunneling amplitude) of the two doublets may be different depending on the exact tunneling site θ on the circumference. As the field is increased, the respective electron densities become similar (pattern changes from standing waves to plane waves), consistent with equal tunnel couplings of the doublets [see Fig. 1(g)].

A striking consequence is the tunability of the level renormalization by $B_\parallel$. Figure 2(a) shows a zoom in the stability diagram of the left shell in Fig. 1(a) at $B_\parallel = 0$ where the onset of inelastic cotunneling processes is clearly observed (see the arrow). The gate dependence of the onset has been explained by tunneling renormalization due to a strongly and a weakly coupled doublet [5,16]. Knowing that the intrashell orbital coupling may induce differently coupled doublets, we can now further test both this simple model and the many-body origin of the gate dependence. As $B_\parallel$ is increased, the couplings to the doublets become equal, and as a result the inelastic cotunneling threshold is expected to gradually become gate
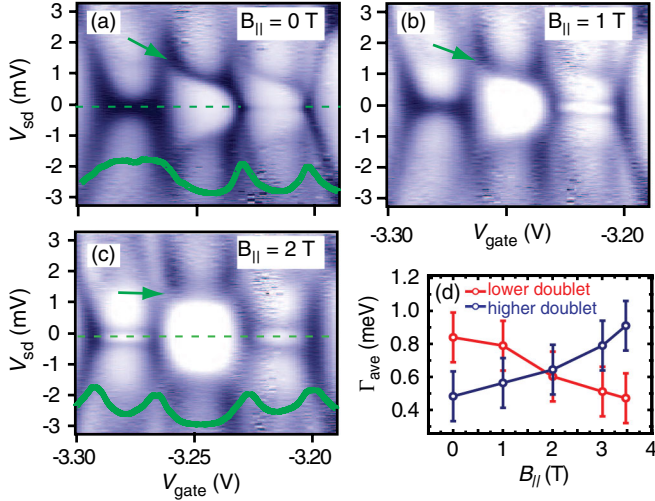
FIG. 2 (color online). (a)–(c) Charge stability diagrams at $B_\parallel = 0, 1, 2$ T showing that the gate dependence (originating from differently coupled doublets) of the inelastic cotunneling threshold vanishes as the parallel field is increased in accordance with the field dependence of the doublet coupling asymmetry [see (d)]. (d) Extracted lead couplings from Coulomb peak widths. (Γ_{ave} at $B_\parallel = 0$ for the lower doublet is a rough estimate, since the fitting formula is not valid in the Kondo regime [11].)

independent. This is indeed observed in the stability diagrams at finite $B_\parallel$, where the gate dependence diminishes for $B_\parallel = 1$ T [Fig. 2(b)] and is absent for $B_\parallel = 2$ T [Fig. 2(c)]. The similar Coulomb peak widths in the linear conductance trace at $B_\parallel = 2$ T indicate that the couplings within the quartet become nearly identical at this field. The $B_\parallel$ dependence of the doublet couplings, estimated from the average width of the two Coulomb peaks belonging to each doublet, is clearly revealed in Fig. 2(d) [11,17].

A more careful analysis of the Coulomb peak widths reveals that the single-shell model does not fully account for all features. At large fields (> 3 T), the coupling of the weakly coupled doublet becomes (even) stronger than that of the strongly coupled doublet [Fig. 1(b)], while the model predicts equal coupling [see Fig. 1(e)]. To fully understand the experimental behavior of the tunnel couplings at large fields, a two-shell model taking into account couplings between levels stemming from different shells must be invoked [18]. Figure 3(c) shows the linear conductance versus $B_\parallel$ and V_{gate} for the gate range shown in Fig. 1(a). An almost identical behavior of Coulomb peaks belonging to the two shells is seen, indicating similar tunnel coupling doublet asymmetries [13]. Furthermore, at larger fields, kinks in the Coulomb peaks and slanted conductance ridges in the Coulomb blockade for filled shells (e.g., filling 4) indicate level crossing behavior, giving rise to the Kondo effect.

For this strongly coupled device, the level structure is best probed by inelastic cotunneling spectroscopy. Figures 3(b), 3(e), and 3(f) show bias spectroscopy plots

versus $B_\parallel$ for different fillings of the shells along the white dashed lines in Fig. 3(c), i.e., one hole (3 electrons), a filled shell, and one electron in the next shell. The observed cotunneling features are understood by considering two nanotube shells separated by a level spacing $\Delta E = E_2 - E_1$, where in addition both shells are split into two doublets due (primarily) to intrashell orbital interaction $\Delta_{KK'1}, \Delta_{KK'2}$ [Fig. 3(a); see also [11]]. As $B_\parallel$ is applied, the doublets within each shell split up, resulting in level crossings between different shells at elevated fields [see Fig. 3(a)]. The thin black lines in Figs. 3(b), 3(c), and 3(f) representing cotunneling excitation, which were obtained from the level spectrum of Fig. 3(a), well reproduce the observed features [19]. The cotunneling data also reveal the presence of an intershell orbital interaction $\Delta_{KK'12}$, which couples orbital states with same spin from different shells, and appears as anticrossings at finite field [e.g., the arrows in Figs. 3(b) and 3(f)]. On the other hand, crossings for states of different spins [e.g., the arrow in 3(f)] indicate that spin-flip scattering is suppressed [20].

The orbital couplings not only modify the internal level structure, but they also induce $B_\parallel$-dependent tunnel couplings, as shown in Fig. 3(d). These effective Γ's are calculated from the eigenstates of the two-shell model using the bare tunnel amplitudes. At zero field, the doublets arrange in strongly and weakly coupled doublets, but as the field is increased, the couplings nonmonotonically approach the original couplings of the shells. (See the horizontal arrows—The valence band shell at larger negative V_{gate} is more strongly coupled, as often seen in nanotubes.) The nonmonotonic coupling behavior is also observed in the data of Fig. 3(c). For instance, the leftmost Coulomb peak in the red square initially broadens and then becomes very narrow at high fields, in agreement with Fig. 3(d) (solid blue line). It is also seen that the tunnel couplings of the inner two doublets in Fig. 3(a) interchange at low fields [see the dotted vertical arrows in Fig. 3(d)], qualitatively consistent with Fig. 3(c), where the widths of the narrowest Coulomb peaks (two leftmost in the red square) become the broadest as the field is increased. Whereas the quantitative details of Fig. 3(d) depend on the phases of the orbital couplings [11], the agreement with the experiment is better assessed by comparing the overall features to an fRG calculation based on the level structure and tunnel couplings.

The fRG calculated linear conductance [7,11] including inter and intrashell orbital couplings, spin-orbit couplings, and the charging energy U_c is shown in Fig. 3(g) [compare to the square in Fig. 3(c)]. Only the relevant and correctly modeled inner four levels are kept. After we choose appropriate intrashell coupling phases, the calculation reproduces the weak and strong Kondo resonances, the non-monotonic magnetic-field dependent Coulomb peak widths, as well as Kondo ridges in Coulomb blockade at finite fields. Interestingly, the finite field Kondo ridges are
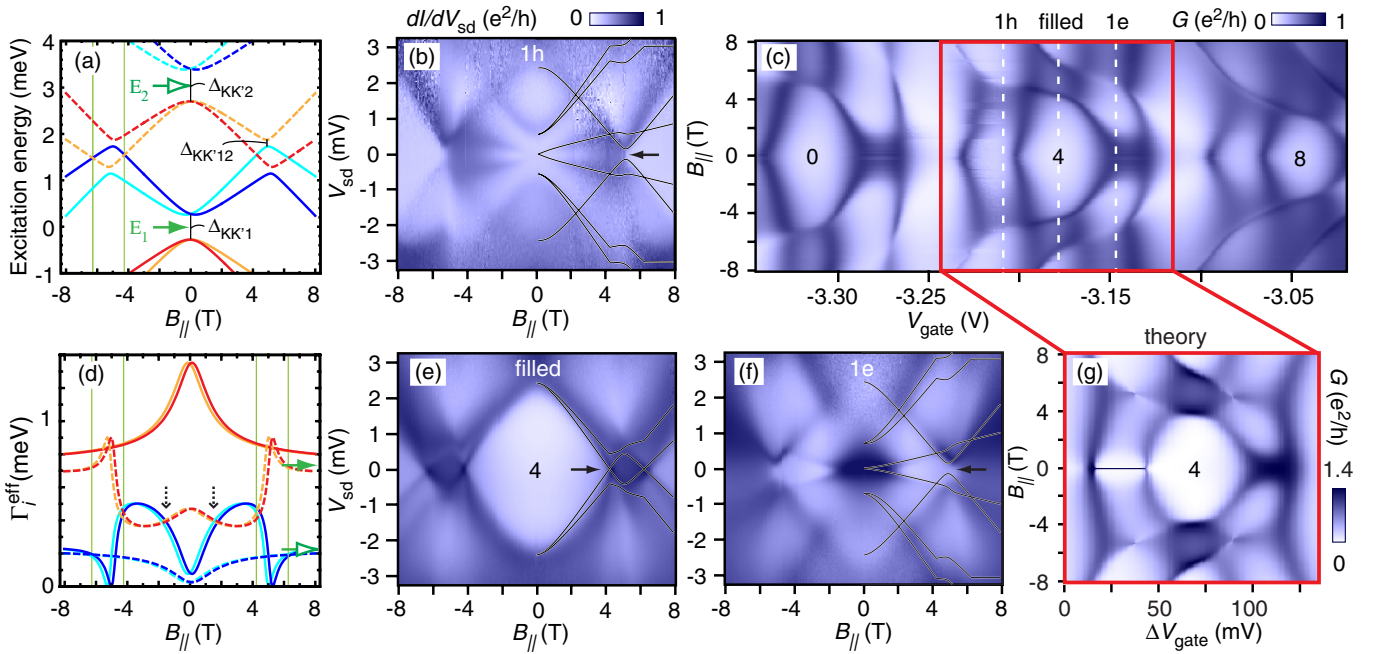
FIG. 3 (color online).   (a) Energy levels of a two-shell model with level crossings (see vertical lines) resulting in finite $B_{\parallel}$ Kondo ridges in (c) for levels having different spins. In contrast, avoided crossings appear at zero (finite) $B_{\parallel}$ due to intrashell (intershell) orbital couplings for levels having same spin. (b) Inelastic cotunneling spectroscopy probing level differences for 1 hole. Lines are fits (to peaks and dips in d^2I/dV_{sd}^2) based on the two-shell model shown in (a). (c) Linear conductance versus $B_{\parallel}$ and V_{gate}, allowing the study of level crossings of states belonging to different shells. (d) Orbital couplings give rise to effective tunnel couplings Γ_i^{eff} of the eigenstates in (a) (horizontal arrows indicate bare shell coupling strengths). Note that we show the sum of the couplings to the left and right leads. The small shift of the couplings within a doublet along $B_{\parallel}$ is due to spin-orbit interaction. (e),(f) As in (b), but for a filled shell (e) and for 1 electron (f). (g) fRG calculation based on the inner four levels of (a) using the corresponding tunnel couplings of (d) [25].

seen to be gate dependent, thus giving rise to a V_{gate} controlled spin ground state transition [21,22] consistent with different tunnel couplings of the states involved [11,23]. Note that, in the $T = 0$ calculation, left-right asymmetric level-lead couplings (corresponding to a higher linear conductance than in the experiment) were chosen to anticipate a suppression at finite T [24].

In conclusion, we have shown that the doublets formed in a nanotube shell in presence of disorder-induced valley mixing may have different tunnel couplings to the leads. Furthermore, this difference is modified by applying a parallel magnetic field. The linear conductance fRG results for a two-shell model show good agreement with experiments.

*k_grove@fys.ku.dk

[1] W. Liang, M. Bockrath, and H. Park, Phys. Rev. Lett. **88**, 126801 (2002).
[2] M. R. Buitelaar, A. Bachtold, T. Nussbaumer, M. Iqbal, and C. Schönenberger, Phys. Rev. Lett. **88**, 156801 (2002).
[3] F. Kuemmeth, S. Ilani, D. C. Ralph, and P. L. McEuen, Nature (London) **452**, 448 (2008).
[4] T. S. Jespersen, K. Grove-Rasmussen, J. Paaske, K. Muraki, T. Fujisawa, J. Nygård, and K. Flensberg, Nature Phys. **7**, 348 (2011).
[5] J. V. Holm, H. I. Jørgensen, K. Grove-Rasmussen, J. Paaske, K. Flensberg, and P. E. Lindelof, Phys. Rev. B **77**, 161406 (2008).
[6] P. Jarillo-Herrero, J. Kong, H. S. J. van der Zant, C. Dekker, L. P. Kouwenhoven, and S. De Franceschi, Nature (London) **434**, 484 (2005).
[7] C. Karrasch, T. Enss, and V. Meden, Phys. Rev. B **73**, 235337 (2006).
[8] D. Goldhaber-Gordon, H. Shtrikman, D. Mahalu, D. Abusch-Magder, U. Meirav, and M. A. Kastner, Nature (London) **391**, 156 (1998).
[9] J. Nygård, D. Cobden, and P. Lindelof, Nature (London) **408**, 342 (2000).
[10] S. De Franceschi, S. Sasaki, J. M. Elzerman, W. G. van der Wiel, S. Tarucha, and L. P. Kouwenhoven, Phys. Rev. Lett. **86**, 878 (2001).
[11] See the Supplemental Material at http://link.aps.org/supplemental/10.1103/PhysRevLett.108.176802 for details on the spinless single-shell model, the two-shell model, and tunneling-induced level renormalization.
[12] Neglecting for now the small spin-orbit interaction.
[13] The narrow Kondo ridges were suppressed in $B_{\parallel}$ sweeps due to a slightly increased T and insufficient resolution.

[14] A. Makarovski, J. Liu, and G. Finkelstein, Phys. Rev. Lett.
99, 066801 (2007).

[15] A. Makarovski, A. Zhukov, J. Liu, and G. Finkelstein,
Phys. Rev. B **75,** 241407 (2007).

[16] K. Grove-Rasmussen, H. I. Jørgensen, B. M. Andersen, J.
Paaske, T. S. Jespersen, J. Nygård, K. Flensberg, and P. E.
Lindelof, Phys. Rev. B **79,** 134518 (2009).

[17] H. I. Jørgensen, T. Novotný, K. Grove-Rasmussen, K.
Flensberg, and P. E. Lindelof, Nano Lett. **7,** 2441 (2007).

[18] A four-shell model is needed to account for the crossing
behavior [11], but the effect on tunnel couplings in a
multishell system is best illustrated in the simpler case
of a two-shell model.

[19] The excitations are calculated from the energy difference
between the ground and excited states in Fig. 3(a).

[20] In the model, the recently understood spin-orbit coupling
identified by the low field and bias behavior [4] is also
included, however, only slightly modifying the energy
spectra.

[21] J. R. Hauptmann, J. Paaske, and P. E. Lindelof, Nature
Phys. **4,** 373 (2008).

[22] N. Roch, S. Florens, V. Bouchiat, W. Wernsdorfer,
and F. Balestro, Nature (London) **453,** 633
(2008).

[23] S. Grap, S. Andergassen, J. Paaske, and V. Meden, Phys.
Rev. B **83,** 115115 (2011).

[24] The narrow $B_\parallel = 0$ Kondo ridge has a small Kondo
temperature and is suppressed in the experiment.

[25] Shell parameters are fixed by the fitting $\{\Delta E, |\Delta_{KK'1}|,$
$|\Delta_{KK'2}|, |\Delta_{KK'12}|, \Delta_{SO}\} = \{3.05, 0.55, 0.7, 0.15, 0.075\}$ meV
and $g_{orb} = 5.1$. Right and left bare couplings
$\{\Gamma_1^L, \Gamma_1^R, \Gamma_2^L, \Gamma_2^R\} = \{0.56, 0.17, 0.17, 0.05\}$ meV, orbital
coupling phases $\{\phi_1, \phi_2, \phi_{12}\} = \{0.85\pi, 0.85\pi, 0\}$, and
$U_c = 4$ meV are used in the fRG calculation.